Synthesis and Characterization of a Novel Bio-Magnetically Recoverable Palladium Nanocomposite for the Photocatalytic Applications

Naeimi, Atena*[+]

Chemistry Department, Faculty of Science, University of Jiroft, Jiroft, I.R. IRAN

Nejat, Razieh

Chemistry Department, Faculty of Science, Kosar University of Bojnord, Bojnord, I.R. IRAN

ABSTRACT: *A novel immobilized sparteine palladium (II) complex on the bio α-Fe_2O_3 nanoparticles was synthesized (Pd-Sparteine- α -Fe_2O_3). XPS, FT-IR, and ICP were used to determine compositional information. TGA* and *VSM*, respectively proved high thermostability and magnetic properties of it. *The size and morphology of this heterogeneous catalyst were investigated using SEM and TEM. Photoluminescence spectrum, BET, DRS, and EDAX of this novel nanocomposite were evaluated for further investigations. The synthesized magnetic nanohybrid was successfully exploited as a new recyclable heterogeneous photocatalyst in the degradation of 2,4- dichlorophenol under visible light irradiation. It exhibited better photocatalytic efficiency of Pd-Sparteine-α-Fe_2O_3 than that of pure iron oxide nanoparticles. This catalyst's high yield and the low reaction time indicated that Pd-Sparteine-α-Fe_2O_3 could be a promising catalyst for direct photocatalyst applications.*

KEYWORDS: *Fe_2O_3, Photocatalyst, 2,4-Dichlorophenol, Water treatment.*

INTRODUCTION

Nowadays, one of the great challenges facing society is finding alternative recoverable catalysts from natural plants to water treatment including the removal of toxic organic compounds and hazardous dyes from wastewaters [1]. While, increasing in these kinds of materials is observed from such as textile, paper, plastic, cosmetic, leather, food, and pharmaceutical industries. On the other hand, the destructive effects on human health or the environment are because governments are forced to pay too much budget to solve these problems. Among several recent strategies for the treatment of water such as physical, chemical, photochemical, and microbiological processes, the photocatalytic technique using unwanted plants is the best one. Because of is inexpensive, naturally abundant, and the reaction produces no environmentally damaging byproducts [2].

The chlorophenols have been listed as toxic pollutants by the Environmental Protection Agency as priority water pollutants. The extensive use of chlorophenol compounds as a fungicide, herbicide, wood preservative, dyes, and drugs and the inability to remove these compounds during

***** *To whom correspondence should be addressed.*
+ *E-mail*: *a.naeimi@ujiroft.ac.it*
1021-9986/2022/1/15-26 *12/$/6.02*

wastewater treatment leads to enhance water pollution. These materials should be removed because they can be extremely dangerous to human health or the environment. Chlorophenols can be removed using conventional processes [3], such as physical, chemical, photochemical, and microbiological processes. Among various methods, the photocatalytic technique has become one of the main routes to degrade organic pollutants into harmless final products [4]. The stable C–Cl bond in chlorophenols, which makes them harmful, is also responsible for their formation of highly toxic by-products during their degradation *via* Advanced Oxidation Processes (AOPs) [5].

Nanocomposite materials as heterogeneous systems, one of the solid constituents traditionally exhibits a nanoscale structure, i.e. one-, two-, or three dimensions of less than 100 nm [6-7]. Supporting metal complexes onto solid supports with high surface area leads to several advantages in comparison to homogenous systems. More facile recovery and more efficiency of the reactions that occurred in the presence of supported metal complexes are among the advantages. However, nanocatalysts, the bridge the gap between heterogeneous and homogeneous catalysis, are very difficult to separate by filtration or precipitation. Thus, magnetic nanoparticles (MAGNPs) can solve this problem due to their large specific surface areas and magnetic properties [8-17].

Bio nanocomposites can attract so much attention leading to interesting physical properties and important potential applications such as water treatment and catalysts industries. Recently, using nanocomposites including metal and metal oxide nanoparticles as heterogeneous nano photocatalysis systems, which can completely treat water in the presence of solar energy as the source of energy and air as an oxidant [18-19]. In this regard, Magnetic ones can easily recycle using an external permanent magnet without the need for filtration, centrifugation, or other tedious workup processes [20-21].

In continuing our work on the synthesis of novel bio nanocomposites based on natural plants for different applications [21-25], here, magnetic iron oxide particles were prepared and modified by (7S, 14aS)-dodecahydro-2H,6H-7,14-methanodipyrido[1,2-a:1',2'-e] [1,5] diazocine (Sparteine) and Pd(II) complex The resulting catalyst is able to degrade 2,4-DCP with excellent yields. The method agrees with the important concepts of green chemistry with the use of inexpensive visible light irradiation and meets the criteria for environmentally friendly procedures. The influence of reaction parameters such as time, pH, and also the reusability of the photocatalyst on the degradation yield have been investigated.

EXPERIMENTAL SECTION

Materials and methods

3-chloropropyltrimethoxysilane, triethylamine, and Sparteine were purchased from Aldrich. All solvents, $FeCl_2.4H_2O$, $FeCl_3.6H_2O$, and $Pd(OAc)_2$ were bought from Merk Company. FT-IR spectra were obtained over the region 400-4000 cm^{-1} with NICOLET IR100 FT-IR with spectroscopic grade KBr. The magnetic properties of Fe_2O_3 and Pd-Sparteine- α-Fe_2O_3 were measured with a vibrating sample magnetometer/ Alternating Gradient Force Magnetometer (VSM/AGFM, MDK Co, Iran, www.mdk-magnetic.com). Inductively coupled plasma (ICP) data are provided by Varian vista-PRO. The field emission scanning electron microscopy (FESEM) analysis was carried out using a Philips XL-300. TEM images were recorded by the Philips cm 30 instrument. X-ray Photoelectron Spectroscopy (XPS) was carried out by the Dual anode (Mg and Al K alpha) achromatic X-ray source. UV-Vis absorption spectra were obtained using Shimadzu UV-2550-8030 spectrophotometer in the range of 190-800 nm with a slit width of 5.0 nm and a light source with a wavelength of 360.0 nm at room temperature. Synthesis of iron oxide nanoparticles was performed by the furnace (FANAZMA GOSTAR).

Green synthesis of iron oxide (α-Fe_2O_3)

A NH_4OH solution (0.01 M) was added to 200 mL of $FeCl_3.6H_2O$ and $FeCl_2.4H_2O$ solution (0.05 M) dropwise (drop rate = 1 mL/min) at room temperature to reach the reaction pH to 11. The mixture of the reaction was heated to 80 °C for 2.5 hours. The resulting α-Fe_2O_3 was separated by an external magnet, washed with water, and dried in an oven under a vacuum. The as-synthesized sample was heated by the furnace at 250 °C for seven hours.

Synthesis of chloro-functionalized _magnetic nanoparticles (Cl@MNs)

Fe_2O_3 (2 g) was sonicated for 1 hour in dry ethanol. Then, 3 chloropropyltrimethoxysilane (2 mL) and triethylamine (0.2 mL) were added to MNs and refluxed for 24 h. The obtained chloro functionalized magnetic nanoparticles

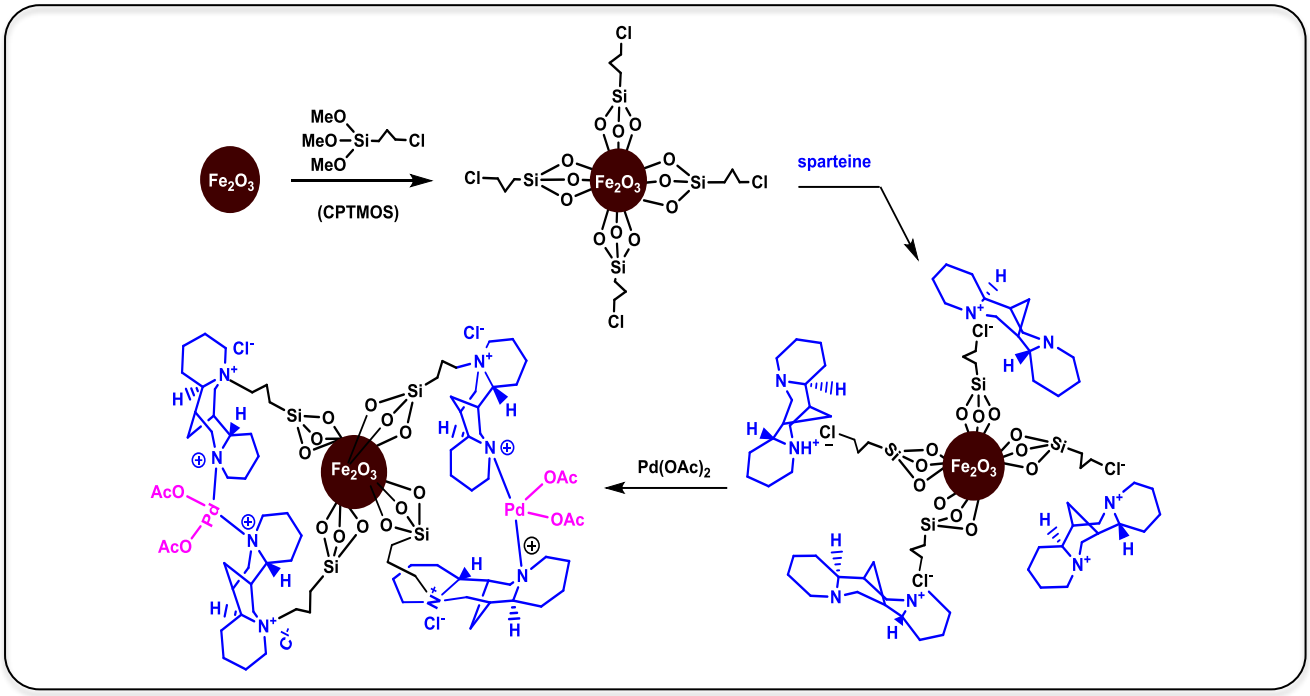

Scheme 1: Preparation procedure of Pd-Sparteine- α -Fe_2O_3.

were separated by an external magnet and washed several times with a mixture of water and ethanol [26].

Synthesis of magnetic nanoparticles supported with (-) sparteine (Sparteine-α-Fe_2O_3)

(-) Sparteine was added to a magnetically stirred mixture of Cl@MNs (3.6 g) in 1,2 dichloroethane (100 mL) and heated to 60 °C. Then, the obtained sparteine- α -Fe_2O_3 was separated using an external magnet.

Synthesis of palladium complex supported on magnetic nanoparticles (Pd-Sparteine- α -Fe_2O_3)

Sparteine- α -Fe_2O_3 (3.3 g) was sonicated in dry 1,2 dichloroethane (30 mL) within 10 min. Then $Pd(OAc)_2$ (0.11 g) was added to this suspension and heated to 60 °C for 24 h under an argon atmosphere. The solid was removed from an external magnetic field and washed (3 × 10 mL) with 1,2 dichloroethane and water [23-29].

RESULTS AND DISCUSSIONS

Characterization of the novel catalyst

The iron oxide nanoparticles were added to 3-chloropropyltrimethoxysilane to obtain chloro-functionalized α-Fe_2O_3 (Cl@MNs). Then, sparteine was reacted with Cl@MNs to have immobilized sparteine on the α -Fe_2O_3 (Sparteine- α -Fe_2O_3). Finally, by adding the $Pd(OAc)_2$ to sparteine- α-Fe_2O_3, palladium- Sparteine complex supported on α -Fe_2O_3 MNPs was formed (Scheme I).

FT-IR spectra of MNs, DABCO, and Pd-Sparteine-α-Fe_2O_3 MNs shown in Fig. 1. In the FT-IR spectrum of MNs, the presence of Fe-O in this nano organic-inorganic hybrid was confirmed by observation of two bands at around 430–600 cm^{-1} [29-33]. In the FT-IR spectrum of DABCO, the observed peaks at 660, 1060, 2960, and 3260 cm^{-1} were related to NC_3, C-C, CH_2, and OH groups, respectively. While, in the FT-IR spectrum of Pd-Sparteine-α-Fe_2O_3, the band at around 2910, 2930, and 1475 cm^{-1} were assigned to the stretching vibrations of CH_2 bond in the Pd-Sparteine- α -Fe_2O_3, respectively [33-34]. Si-O stretching bond was confirmed at about 900- 1200 cm^{-1}. The presence of C-N^+ stretching at 1615 cm^{-1} in the spectrum of Pd-Sparteine-α-Fe_2O_3 [34] was shown the anchoring of (-) Sparteine on Cl@ α -Fe_2O_3. In the spectrum of Pd-Sparteine- α -Fe_2O_3, the appeared peaks at 1365 and 1577 cm^{-1} for COO (in acetate) [27] were related to the presence of Pd in the catalyst.

The magnetic properties of MNs and Pd-Sparteine-α -Fe_2O_3 were characterized by a vibrating sample magnetometer (VSM) at room temperature (Fig.2). MNs are superparamagnetic and the value of saturation magnetic moments of iron oxide nanoparticles is 57.6 emu/g. While Pd-Sparteine- α -Fe_2O_3 displayed a paramagnetic

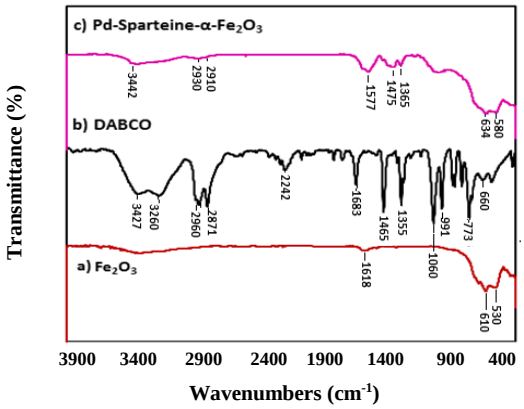

Fig. 1: The FT-IR spectra of a) α -Fe_2O_3, b) DABCO, and c) Pd-Sparteine-α-Fe_2O_3.

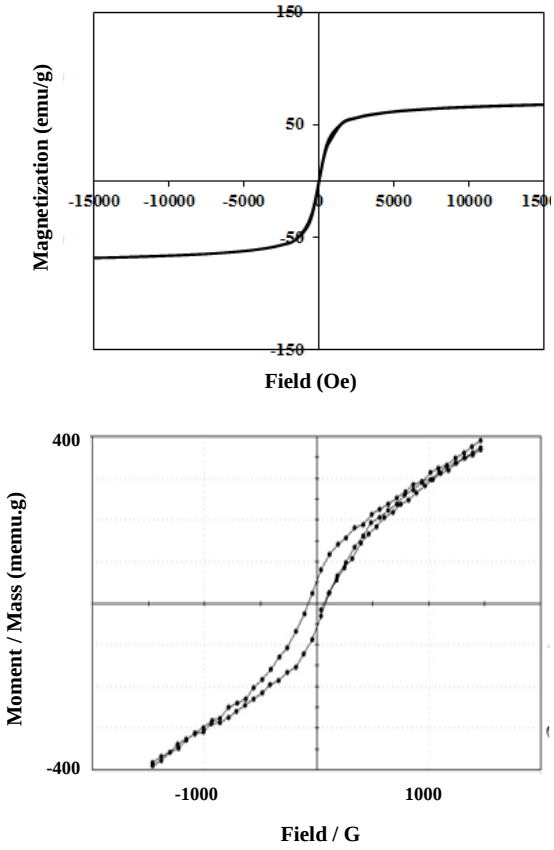

Fig. 2: The vibrating sample magnetometer (VSM) of MNs (top) and Pd-Sparteine- α -Fe_2O_3 (down).

behavior, as evidenced by a zero coercivity on the magnetization loop. The saturation magnetizations of Pd-Sparteine- α -Fe_2O_3 was 400 memu/g, respectively [36]. XPS, an important technique to give information about the surface elements, was also carried out for Pd-Sparteine-

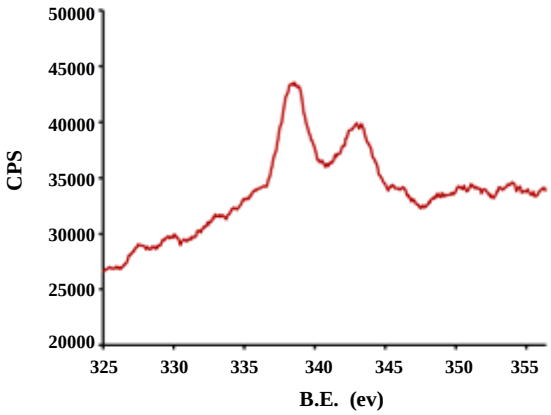

Fig. 3: XPS spectrum of Pd-Sparteine- α -Fe_2O_3.

α -Fe_2O_3 (Fig. 3). X-ray Photoelectron Spectroscopy (XPS) helped determine the oxidation state of the Pd surface in the catalyst. The binding energy curve showed a double peak at 337.3 eV (3d5/2) and 343 eV (3d3/2) which could be attributed to Pd (II) for the brown catalyst [37].

Fig. 4 shows the Transmission Electron Microscopy (TEM) of Pd-Sparteine- α -Fe_2O_3. This image showed that the average size of these particles is less than 40 nm (Fig. 4a). The SEM image of Pd-Sparteine- α -Fe_2O_3 showed uniformity and spherical morphology of nanoparticles (Fig. 4 b). On the other hand, the prevention of aggregation of MNs was observed by modification of it by the Pd complex (Fig. 4c).

The EDAX analysis confirmed the presence of O, C, N, Fe, Si, and Pd in the Pd-Sparteine-α-Fe_2O_3 sample (Fig. 5)

The reflection planes of (2 2 0), (3 1 1), (4 0 0), (4 2 2), (5 1 1) and (4 4 0) at around 2θ = 30.4°, 35.8°, 43.6°, 53.7°, 57.6°and 63.2° were readily recognized from the XRD pattern of MNs and Pd-DABCO-α-Fe_2O_3 (Fig. 6) [26]. The observed diffraction peaks agree with JCPDS file No 89-8103. The same set of characteristic peaks was observed in the XRD pattern of Pd-Sparteine- α -Fe_2O_3, which indicates the stability of the crystalline phase of nanoparticles during the subsequent surface modification (Fig. 6) [30].

Thermostability of the MNs and Pd-Sparteine-α-Fe_2O_3 were considered by thermogravimetric analysis using the powder sample under a nitrogen atmosphere (Fig. 7). TGA curve of MNs shows the small amount of weight loss around 200 °C was attributed to the desorption of adsorbed water (Fig. 7a). Another mass loss appeared at around 400 °C and the organic parts decomposed completely at 800 °C. While, TG curve indicates that Pd-Sparteine- α -Fe_2O_3 showed a weight loss of about 1.2 % between 25 °C to 185 °C, which removal of adsorbed water and solvent molecules

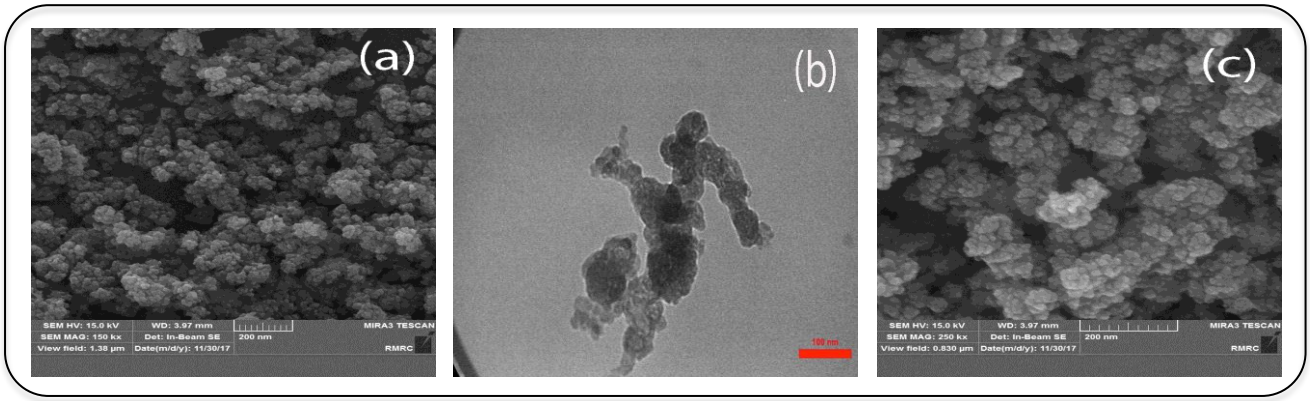

Fig. 4: SEM image Pd-Sparteine- α -Fe_2O_3 (a), TEM image of Pd-Sparteine- α -Fe_2O_3 (b), and SEM image of MNs.

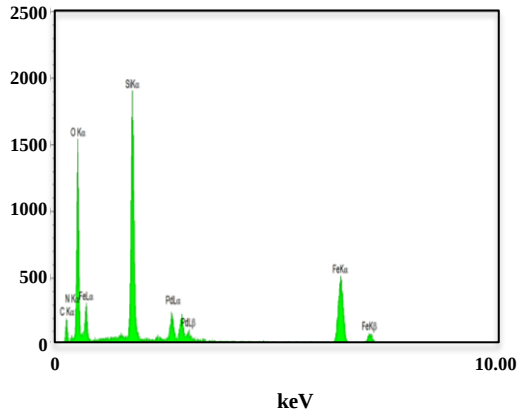

Fig. 5: EDAX image of Pd-Sparteine-α-Fe_2O_3.

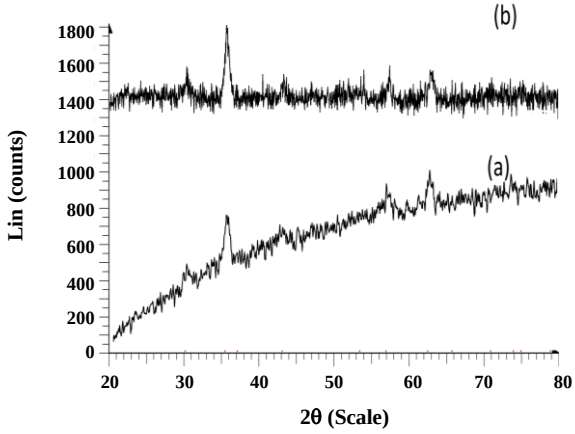

Fig. 6: XRD of a) MNs and b) Pd-Sparteine- α -Fe_2O_3.

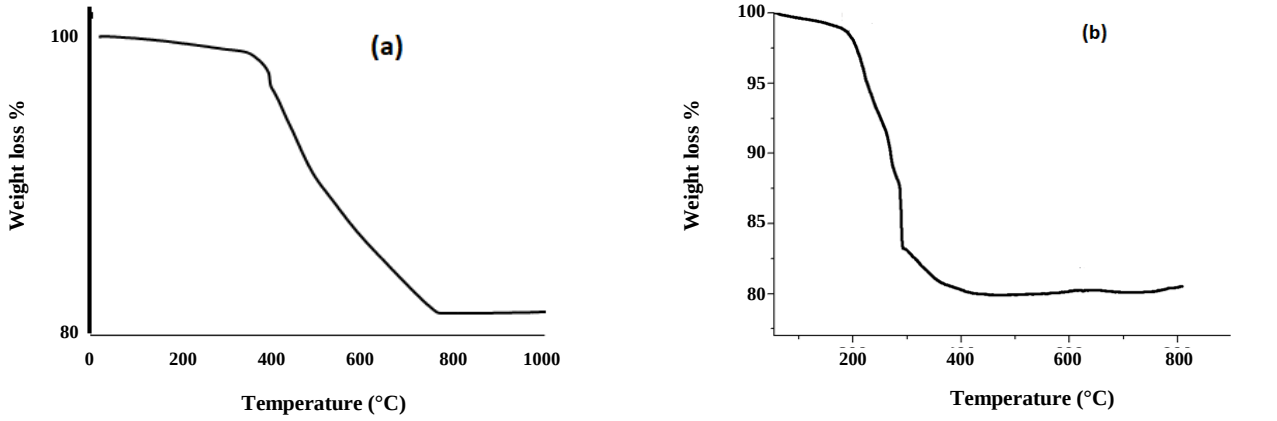

Fig. 7: Thermogravimetric analysis of a) MNs and b) the Pd-Sparteine- α -Fe_2O_3.

were shown (Fig. 7b). On the other hand, the TG curve shows a mass loss, about 20.1%, in the temperature range from 185 to 640 °C, which is related to the decomposition of the organically modified framework. The loss centered at higher temperatures should be attributed to the desorption of several organic species**.**

The bandgap energy of 2.35 eV estimated by the diffuse reflectance spectroscopy (DRS) for Pd-Sparteine-

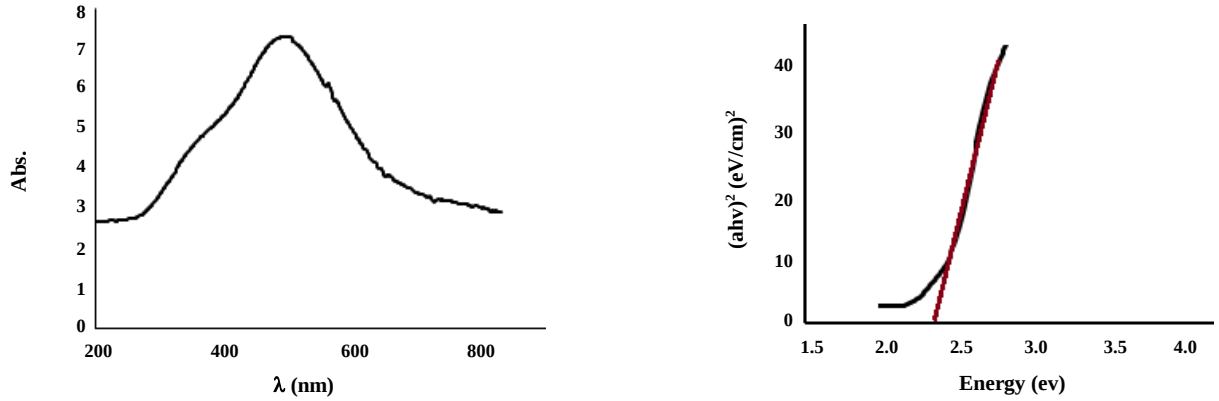

Fig. 8: DRS spectra of the Pd-Sparteine-α-Fe_2O_3.

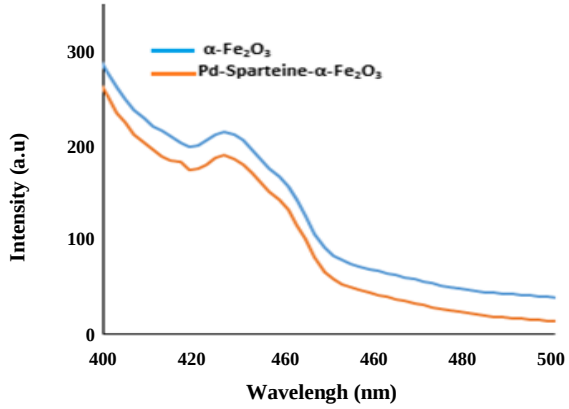

Fig. 9: PL spectra of the a) MNs and b) Pd-Sparteine-α-Fe_2O_3.

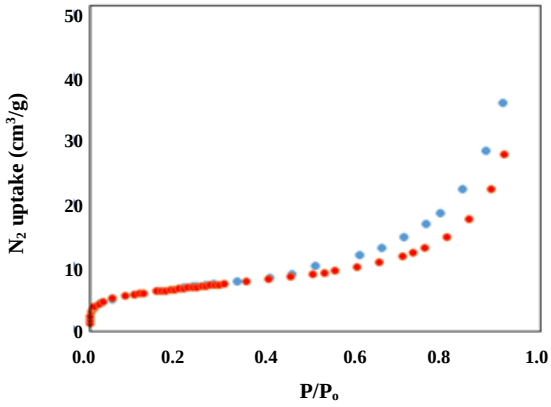

Fig. 10: BET surface areas, pore volumes, and pore diameters of Pd-Sparteine-α-Fe_2O_3.

α-Fe_2O_3, exhibited that this product can be appropriate for photocatalytic activity in the visible region of the solar spectrum (Fig. 8).

Photoluminescence spectra give a glimpse into the separation and recombination of photogenerated charge carriers for various transitions. The PL intensities of α-Fe_2O_3 and Pd-Sparteine-α-Fe_2O_3 are shown in Fig. 9. The PL intensity of pure α-Fe_2O_3 is high when compared to Pd-Sparteine-α-Fe_2O_3. Thus recombination reactions are reduced considerably in the Pd-Sparteine-α-Fe_2O_3.

The specific surface area of Pd-Sparteine-α-Fe_2O_3 was measured using the BET method. As can be seen from Fig. 10, the BET surface area of the prepared nanostructure is 39.8 m^2/g. The pore volume and pore diameter were calculated by the BJH method for catalysts and the values are presented in Table 2.

On the other hand, the Pd content was about 0.17 mmol on 1.0 g of Pd-Sparteine-α-Fe_2O_3, according to inductively coupled plasma optical emission spectroscopy (ICP/OES) analysis.

Photocatalytic degradation of 2,4-DCP

The photocatalytic activities of Pd-Sparteine- α -Fe_2O_3 are evaluated by taking 0.1 g of catalyst and 50 mL of the reaction mixture of 2,4-DCP (20 mg/L) in an aqueous medium. For having adsorption/desorption equilibrium between the pollutant and the surface of the catalyst, the 2,4-dichlorophenol molecular was kept in the dark under magnetic stirring for 30 min. The visible illumination was provided by a 400 W lamp (high-pressure mercury-vapor lamp and λ=546.8 nm and an air diffuser (air pump, flow: 3.5 L/min) was located at the bottom of the reactor to uniformly disperse air into the solution. The photocatalytic reaction temperature was kept at room temperature using cooling fans to prevent any thermal catalytic effect. The UV-Visible absorption spectrum of the 2,4-DCP degradation shows in Fig. 11.

Table 2: BET surface areas, pore volumes, and pore diameters of Pd-Sparteine-α-Fe_2O_3.

Sample	BET surface area ($m^2.gr^{-1}$)	Pore volume ($cm^3.gr^{-1}$)	Pore diameter (nm)
Pd-Sparteine-α-Fe_2O_3	39.8.	0.24	3.1

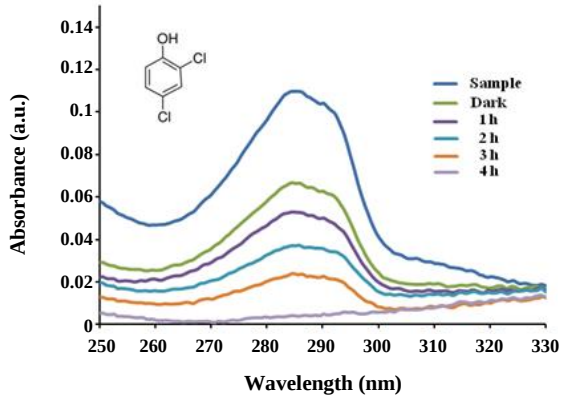

Fig. 11: UV- Visible absorption spectra of the 2,4-DCP degradation in the presence of Pd-Sparteine- α -Fe_2O_3 ([2,4-DCP] =20 mg/L, [catalyst]= 0.1 g and pH=5.0).

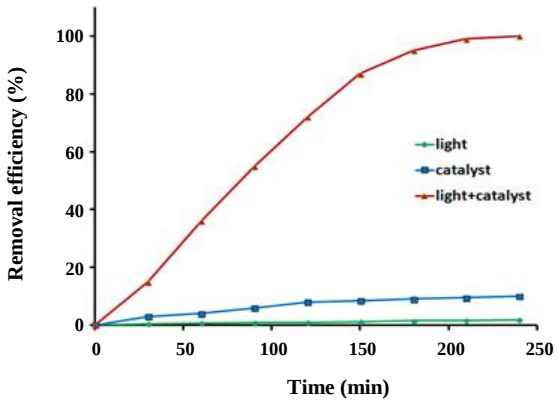

Fig. 12: Effects of light, catalyst, and (light+catalyst) on the 2,4-DCP degradation.

Fig. 11 shows the UV-Visible absorption spectra α of the 2,4-DCP degradation in the presence of Pd-Sparteine- α -Fe_2O_3 under visible light. It should be noted that the peak at 285 nm is related to 2,4-DCP. The intensity of the characteristic peak decreases with the irradiation time and tends to disappear after 4 h illumination indicating the 2,4-DCP can be photodegraded effectively by photocatalyst [37-38].

Optimization of reaction conditions

Preliminary, in order to investigate the catalytic performance of Pd-Sparteine-α-Fe_2O_3, we examined it as a catalyst in 2,4-DCP degradation. Various conditions on the yield of 2,4-DCP degradation were studied using catalyst loading, the presence of light irradiation compared with dark, and the presence of catalyst compared with the pristine α-Fe_2O_3, and various pH. It was found that the degradation produces the best yield under visible-light irradiation in water using 0.1 g of catalyst in pH=5. A decrease in the amount of catalyst leads to a decrease in yield and the yield remained almost unaffected when the catalyst loading was increased to 0.2 g.

The effects of the presence of catalyst and light irradiation on 2,4-DCP degradation were investigated (Fig. 12). Degradation of 2,4-DCP did not happen in the absence of a photocatalyst under visible light irradiation. The partial value of 2,4-DCP concentration (about ~10%) is reduced after running the photocatalytic reaction in the dark, which can be referred to as the partial adsorption of organic molecules on the surface of photocatalyst particles. Degradation efficiency was enhanced up to 100% when the 2,4-DCP solution containing photocatalyst was exposed to visible light irradiation.

Furthermore, the α -Fe_2O_3 was used as a photocatalyst for the degradation of 2,4-DCP in an aqueous system. Fig. 13 shows that the photoactivity of the Pd-Sparteine- α -Fe_2O_3 photocatalyst is far higher than α -Fe_2O_3 photocatalyst.

The effect of the initial pH of water on the 2,4-DCP was investigated at pH 3, 5, and 8 (Fig. 10) using 0.01 mol/L HCl and NaOH, respectively. The high surface area of nanoparticles plays a significant role as the reaction takes place. It seems that the acid-base condition of the photocatalyst surfaces can have a large impact on the adsorption-desorption and photocatalytic degradation performance [40]. Fig. 14 depicts the percentage degradation as a function of pH. The catalyst surfaces are positive and negative charges in the presence of alkaline and acidic media. At slightly acidic conditions (pH=5), the best degradation was obtained and further increases in pH resulted in lower removal efficiency.

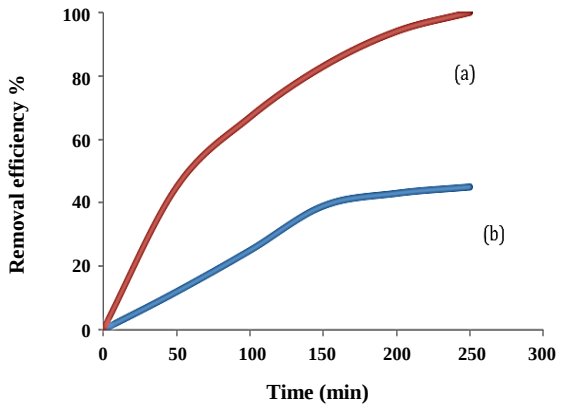

Fig. 13: The removal percentage of 2,4-DCP in the presence of α -Fe_2O_3 (b) and Pd-Sparteine- α -Fe_2O_3 (a).

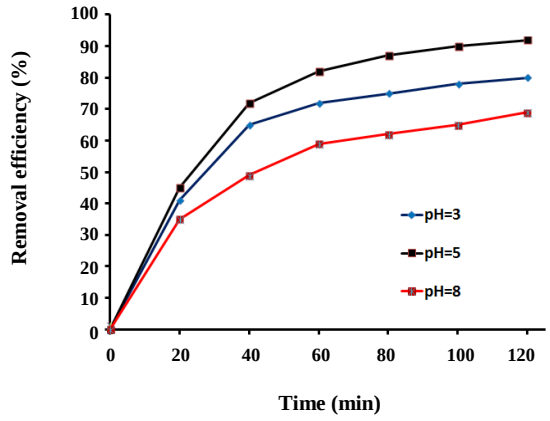

Fig. 14: Effect of the solution pH for the 2,4-DCP degradation in presence of the of Pd-Sparteine- α -Fe_2O_3.

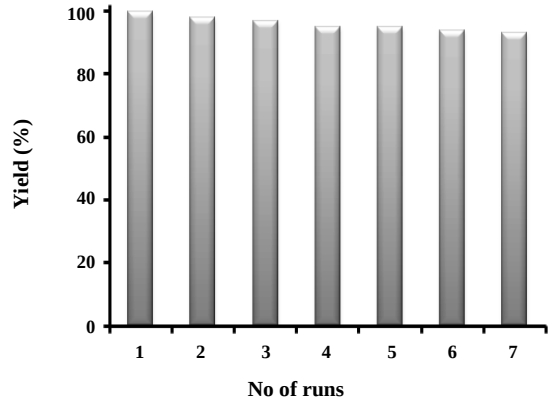

Fig. 14: Reusability of the of Pd-Sparteine- α -Fe_2O_3 for the 2,4-DCP degradation.

The reusability of Pd-Sparteine-Fe_2O_3 was investigated for 2,4- chlorophenol photodegradation under optimized conditions (Fig. 15) [40-42]. After completing the reaction, the catalyst was separated by one magnet and washed with deionized water. It can directly carry forward to the next reaction [43]. As shown in Fig. 15, after the seventh run, a significant decrease in its activity of it was not observed.

The tentative mechanism of this photo-oxidation of 2,4 DCP using this bio-nano photocatalyst based on hydroxyl radical intervention was proposed in Fig. 16. The removal of an ortho and para chlorine attached to 2,4-DCP would give rise to 4-CP and 2-CP, respectively [44-47].

Moreover, isopropanol can be used as a hydroxyl radicals' scavenger, and the rate constant of reaction of these radicals on isopropanol is close to 2×10^9 M^{-1} s^{-1} [48]. We added isopropanol (2.0%) as a hydroxyl radicals' scavenger to 2,4-DCP and Pd-Sparteine-α-Fe_2O_3 suspension under light irradiation. Therefore, since photodegradation of the 2,4-DCP was inhibited, the degradation of 2,4-DCP can be directly attributed to the attack of ˙OH radicals.

Finally, we compared the catalytic activities of this nano-bio-photocatalyst and other very recent photocatalysts for 2,4-DCP degradation under visible light (Table 2). The good dispersibility of nanostructure of Pd-Sparteine- α -Fe_2O_3bio-nanocomposite in water, due to its lightweight and low density shows the best degradation of 2,4-DCP in minimum times. However, the high dispersibility, larger surface area as well as pore volume, and good surface permeability made it cheap and efficient for adsorption of 2,4-DCP.

CONCLUSIONS

In summary, palladium- Sparteine complex supported on Fe2O3 magnetic nanoparticles as a magnetically heterogeneous catalyst was synthesized. Its photocatalytic activity was investigated in the degradation of 2,4-DCP under visible light irradiation. The catalyst was easily isolated from the reaction mixture by an external magnet and reused at least seven times without significant degradation in its activity. This catalyst is a good candidate for performing the degradation of organic pollutants of the water.

Table 2: Comparison of adsorption performance for 2,4-DCP using Pd-Sparteine- α -Fe_2O_3 and other adsorbents reported in the literature.

Entry	Catalyst	Time/min	Degradiation%	Reference
1	Pd-Sparteine-α-Fe_2O_3 bio nanocomposite	240	100	This work
2	TiO_2	180	26	8
3	AgCoTC	180	60	8
4	SBA-CIL-CS-Lac	2100	90	7
5	Ni/Fe bimetal	240	74	17
6	CSPs	240	68	18
7	Pal-Fe/Ni	240	80	19
8	CdTe/CdS/N-rGO	360	70	20

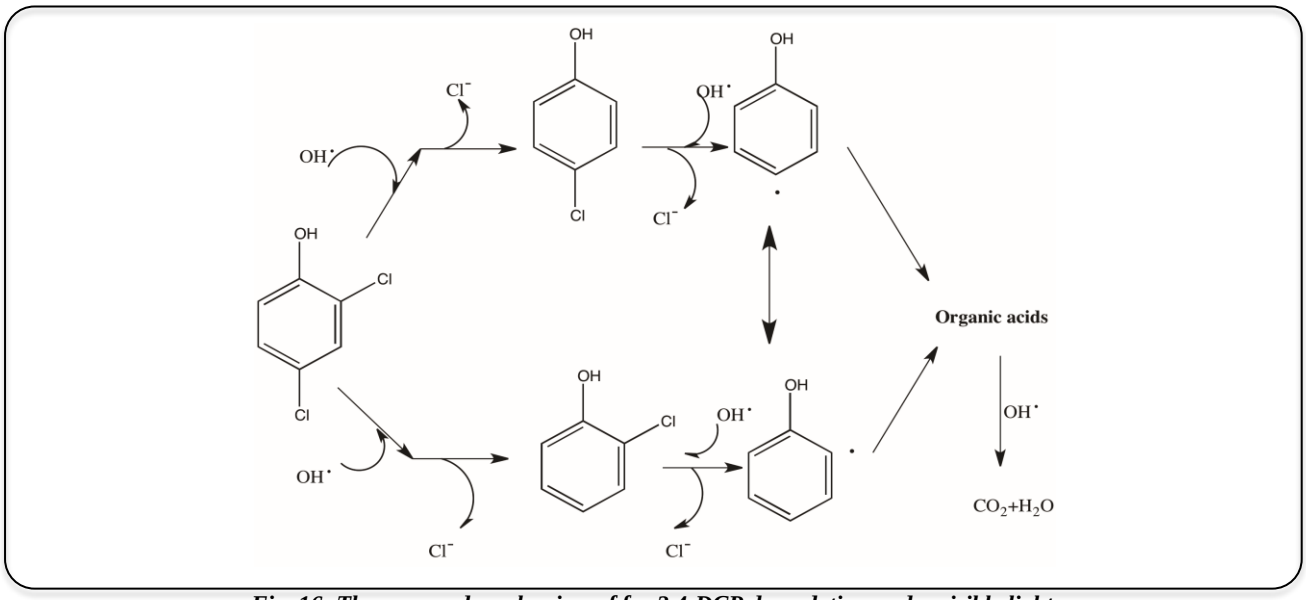

Fig. 16: The proposed mechanism of for 2,4-DCP degradation under visible light.

Acknowledgments

Financial support for this work by the University of Jiroft and Kosar University of Bojnord is gratefully acknowledged.

Received : Jan. 13, 2021 ; Accepted : Apr. 5, 2021

REFERENCES

[1] Kachbouri S., Elaloui E., Moussaou Y., The Effect of Surfactant Chain Length and Type on the Photocatalytic Activity of Mesoporous TiO_2 Nanoparticles Obtained *via* Modified Sol-Gel Process, *Iranian Journal of Chemistry and Chemical Engineering (IJCCE)*, **38(1)**: 17-26 (2019).

[2] Rani B., Punniyakoti S., Sahu N.K., Polyol Asserted Hydrothermal Synthesis of SnO_2 Nanoparticles for the Fast Adsorption and Photocatalytic Degradation of Methylene Blue Cationic Dye, *New J. Chem.*, **42**: 943–954 (2018).

[3] Abdelhameed R.R., Abdel-Gawad H.A., Hegazi B., Effective Adsorption of Prothiofos (O-2,4-dichlorophenyl O-ethyl S-propyl phosphorodithioate) from Water Using Activated Agricultural Waste Microstructure, *J. Environ. Chem. Eng.*, **8**: 103768 (2020).

[4] Khan H., Usen N., Boffito D., Spray-dried Microporous Pt/TiO_2 Degrades 4-chlorophenol under UV and Visible Light, *J. Environ. Chem. Eng.*, **7**: 103267 (2019).

[5] Wang W., Lee G.J., Wang P., Qiao Z., Liu N., Wu J.J., Microwave Synthesis of Metal-Doped ZnS Photocatalysts and Applications on Degrading 4-Chlorophenol Using Heterogeneous Photocatalytic Ozonation Process, *Sep. Purify. Technol.*, **237**: 116469 (2020).

[6] Bhattacharjee A., Ahmaruzzaman M., Devi T.B., Nath J., Photodegradation of Methyl Violet 6B and Methylene Blue Using Tin-Oxide Nanoparticles (Synthesized *via* a Green Route), *J. Photochem. Photobiol. A Chem*.,**325**: 116–124 (2016).

[7] Qiu X, Qin J, Xu M, Kang L, Hu Y Organic-Inorganic Nanocomposites Fabricated *via* Functional Ionic Liquid as the Bridging Agent for Laccase Immobilization and Its Application in 2,4-Dichlorophenol Removal, *Colloid Surf. B Biointerfaces*, **179**: 260-269(2019).

[8] Monazzam P., Pirbazari,A. Khodaee E. Z., Enhancement of Visible Light Photoactivity of Rutile-Type TiO_2 by Deposition of Silver onto Co-TiO_2/MWCNTs Nanocomposite for Degradation of 2,4-dichlorophenol, *Mater. Chem. Phys*. **228**: 263-271(2019).

[9] Qiu X., Qin J., Xu M., Kang L., Hu Y., Organic-Inorganic Nanocomposites Fabricated Via Functional Ionic Liquid as the Bridging Agent for Laccase Immobilization and Its Application in 2,4-Dichlorophenol Removal, *Colloids Surf. B: Biointerfaces*, **179**: 260-269 (2019).

[10] Abdi V., Sourinejad I., Yousefzadi M., Ghasemi Z., Mangrove-Mediated Synthesis of Silver Nanoparticles Using Native Avicennia Marinaplant Extract from Southern Iran, *Chem. Eng. Commun*., **205**: 1069-1076(2018).

[11] Abdi V., Sourinejad I., Yousefzadi M., Ghasemi Z., Biosynthesis of Silver Nanoparticles from the Mangrove Rhizophora mucronata: Its Characterization and Antibacterial Potential, *Iranian Journal of Science and Technology, Transactions A: Science*, **43**: 2163–2171(2019).

[12] Ghasemi Z., Abdi V., Sourinejad I., Single-Step Biosynthesis of Ag/AgCl@TiO2 Plasmonic Nanocomposite with Enhanced Visible Light Photoactivity Through Aqueous Leaf Extract of a Mangrove Tree, *Appl. Nanosci.*, **10:** 507-516 (2020).

[13] Moradi N., Amin M.M., Fathizadeh A., Ghasemi Z., Degradation of UV-Filter Benzophenon-3 in Aqueous solution Using TiO_2 Coated on Quartz Tubes, *J. Environ. Health Sci. Eng*, **16**: 213-228 (2018).

[14] Aghajari N., Ghasemi Z., Younesi H., Bahramifar N., Synthesis, Characterization and Photocatalytic Application of Ag-Doped Fe-ZSM@TiO_2 Nanocomposite for Degradation of Reactive Red 195 (RR 195) in Aqueous Environment under Sunlight Irradiation, *J. Environ. Health Sci. Eng.*, **17**: 219-232. (2019).

[15] Gnanaprakasam A. J., Sivakumar V. M., Thirumarimurugan M., Investigation of Photocatalytic Activity of Nd-Doped ZnO Nanoparticles Using Brilliant Green Dye: Synthesis and Characterization, *Iranian Journal of Chemistry and Chemical Engineering (IJCCE)*, **37(2)**: 61-67 (2018).

[16] Malekhosseini H., Mahanpoor K., Khosravi M., Motiee F., Kinetic Modeling and Photocatalytic Reactor Designed for Removal of Resorcinol in Water by Nano $ZnFe_2O_4$/Copper Slag as Catalyst: Using Full Factorial Design of Experiment, *Iranian Journal of Chemistry and Chemical Engineering (IJCCE)*, **38(3)**: 257-266 (2019).

[17] Zheng K., Song Y., Wang X., Li X., Mao X., Wang D., Understanding the Electrode Reaction Process of Dechlorination of 2,4-dichlorophenol over Ni/Fe Nanoparticles: Effect of pH and 2,4-dichlorophenol Concentration, *J. Environ. Sci*., **84**: 13-20 (2019)

[18] Zhou L., Xu Z., Yi K., Huang Q., Chai K., Tong Z., Ji H., Efficient Remediation of 2,4-dichlorophenol from Aqueous Solution Using β-cyclodextrin-based Submicron Polymeric Particles, *Chem. Eng. J.*, **360**: 531-541(2019).

[19] Ezzatahmadi N., Millar G. J., Ayoko G. A., Zhu J., Zhu R., Liang X., He H., Xi Y., Degradation of 2,4-Dichlorophenol Using Palygorskite-Supported Bimetallic Fe/Ni Nanocomposite as a Heterogeneous catalyst, *Appl. Clay Sci*., **168**: 276-286 (2019).

[20] Chongyang L., Jinze L., Linlin S., Yaju Z., Chun L., Huiqin W., Pengwei,H. Changchang M., Yongsheng Y., Visible-Light Driven Photocatalyst of CdTe/CdS Homologous Heterojunction on N-rGO Photocatalyst for Efficient Degradation of 2,4-dichlorophenol, *J. Taiwan Institut. Chem. Engin*., **93:** 603-615 (2018).

[21] Tajik E., Naeimi A., Amiri A., Fabrication of Iron Oxide Nanoparticles, and Green Catalytic Application of an Immobilized Novel Iron Schiff on Wood Cellulose, *Cellulose*, **25**: 915–923(2018).

[22] Naeimi A., Amiri A., Ghasemi Z., A Novel Strategy for Green Synthesis of Colloidal Porphyrins/Silver Nanocomposites by Sesbania Sesban Plant and Theircatalytic Application in the Clean Oxidation of Alcohols, *J. Taiwan Inst. Chem. Eng.*, **80**: 107–113(2017).

[23] Honarmand M., Naeimi A., Zahedifar M., Nanoammonium salt: a Novel and Recyclable Organocatalyst for One-Pot Three-Component Synthesis of 2-amino-3-cyano-4H-pyran Derivatives, *J. Iran Chem. Soc.* **14**: 1875–1888 (2017).

[24] Naeimi A., Payandeh M., Ghara A.R., Ghadi F.E., In vivo Evaluation of the Wound Healing Properties of Bio-Nanofiber Chitosan/ Polyvinyl Alcohol Incorporating Honey and *Nepeta dschuparensis*, *Carbohydr. Polym*., **240**: 116315 (2020).

[25] Naeimi A., Abbasspour S., Torabizadeh S.A., The First and Low Cost Copper Schiff Base/ Manganese Oxide Bio Nanocomposite from Unwanted Plants as a Robust Industrial Catalyst, *Artif. Cells Nanomed. Biotechnol*., **48**: 560-571 (2020).

[26] Sobhani S., Pakdin-Parizi Z., Palladium-DABCO Complex Supported on Fe_2O_3 Magnetic Nanoparticles: A New Catalyst for C-C Bond Formation viaMizoroki-Heck Cross- Coupling Reaction, *Appl Catal A.* **479**: 112-120 (2014).

[27] Tang B.Z., Geng Y., Lam J.W.Y., Li B., Jing X., Wang X., Wang F., Pakhomov A.B., Zhang X.X., Processible Nanostructured Materials with ElectricalConductivity and Magnetic Susceptibility: Preparation and Properties of Maghemite/Polyaniline Nanocomposite Films, *Chem Mater*., **11**: 1581-1589 (1999).

[28] Jensen D.R., Pugsley J.S., Sigman M.S., Palladium-Catalyzed Enantioselective Oxidations of Alcohols Using Molecular Oxygen, *J. Am. Chem. Soc*., **123**: 7475-7476 (2001).

[29] Das S., Bhunia S., Maity T., Koner S., Suzuki Cross-Coupling Reaction over Pd-Schiff-Base Anchored Mesoporous Silica Catalyst, *J. Mol. Catal. A. Chem*., **394**: 188-197 (2014).

[30] Sobhani S., Bazrafshan M., Arabshahi D.A., Pakidn P.Z., Phospha-Michael Addition of Diethyl Phosphite to α,β-unsaturated Malonates Catalyzed by Nanoγ-Fe_2O_3-Pyridine Based Catalyst as a New Magnetically Recyclable Heterogeneous Organic Base, *Appl. Catal. A. Gen.*, **454**: 145-151(2013).

[31] Hasaninejad A., Shekouhy M., Golzar N., Zare A., Doroodmand M.M., Silica Bonded n-propyl-4-aza-1-azoniabicyclo[2.2.2]octane Chloride (SBDABCO): A Highly Efficient, Reusable and New Heterogeneous Catalyst for the Synthesis of 4H-benzo[b]pyran Derivatives, *Appl Catal A.*, **402**: 11-22 (2011).

[32] Mukhopadhyay K., Sarkar B.R., Chaudhari, R.V. Anchored Pd Complex in MCM-41 and MCM-48: Novel Heterogeneous Catalysts forHydrocarboxylation of Aryl Olefins and Alcohols, *J. Am. Chem. Soc*., **124**: 9692-9693 (2002).

[33] Wei L., Tian, Y. Li P., Zhang B., Zhang H., Geng W., Zhang Q., Synthesis of Rattle-Type Magnetic Mesoporous Fe_3O_4@mSiO_2@BiOBr Hierarchical Photocatalyst and Investigation of Its Photoactivity in the Degradation of Methylene Blue, *RSC Adv*., **5**: 48050-48059 (2015).

[34] Ghasemi E., Ziyadi H.L., Afshar A.M.L., Sillanpaa M., Iron Oxide Nanofibers: A New Magnetic Catalyst for Azo Dyes Degradation in Aqueous Solution, *Chem. Eng. J.*, **264**: 146-151 (2015).

[35] Nejat R., Mhajoub A.R., Hekmatian Z., Akhadbakht A., Pd-Functionalized MCM-41 Nanoporous Silica as an Efficient and Reusable Catalyst for Promoting Organic Reaction, *RSC Adv.*, **5**: 16029-16035(2015).

[36] Sobhani S., Hosseini Moghadam H., Skibsted J. Sansano J. M. A Hydrophilic Heterogeneous Cobalt Catalyst for Fluoride-Free Hiyama, Suzuki, Heck and Hirao Cross-Coupling Reactions in Water, *Green Chem*. **22**, 1353-1365 (2020).

[37] Abolhosseini S.A., Mahjoub A.R., Eslami-Moghadam M., Fakhri H., Dichloro (1,10-phenanthroline-5,6-dione) Palladium (II) Complex Supported Bymesoporous Silica SBA-15 as a Photocatalyst for Degradation of 2,4-dichlorophenol, *J. Mol. Struct*. **1076**: 568-575(2014).

[38] Bell A.T., The Impact of Nanoscience on Heterogeneous Catalysis. *Science*, **299**: 1688-1691 (2003).

[39] Chen D., Ray A.K., Photodegradation Kinetics of 4-Nitrophenol in TiO_2 Suspension, *Water Res.*, **32**: 3223-3224(1998).

[40] Zolfigol M.A., Azadbakht T., Khakyzadeh V., Nejatyami R., Perrin D.M., C(sp2)–C(sp2) Cross Coupling Reactions Catalyzed by an Active and Highlystable Magnetically Separable Pd-Nanocatalyst in Aqueous Media, *RSC Adv*. **4**: 40036-40042(2014).

[41] Rossi L.M., Costa N.J.S., Silva F.P., Wojcieszak R., Magnetic Nanomaterials in Catalysis: Advanced Catalysts for Magnetic Separation and Beyond, *Green Chem.*, **16**: 2906-2933 (2014).

[42] Kazemi M., Ghobadi M., Mirzaie A., Based on Cobalt Ferrite Nanoparticles ($CoFe_2O_4$ MNPs) as Catalyst and Support: Magnetically Recoverable Nanocatalysts in Organic Synthesis, *Nanotechnol. Rev.*, **7**: 43-68(2017).

[43] Wang Z., Yu Y., Zhang Y.X., Li S.Z., Qian H., Lin Z.Y., A Magnetically Separable Palladium Catalyst Containing a Bulky N-Heterocyclic Carbene Ligandfor the Suzuki–Miyaura Reaction, *Green Chem.*, **17**: 413-420(2015).

[44] Richard C., Boule P., Oxidizing Species Involved in Transformations on Zinc Oxide. *J. Photochem. Photobiol. A Chem.*, **60**: 235–243(1991).

[45] Shahrnoy A.A., Mahjoub A.R., Morsali, Dusek A.M.V., Eigner Sonochemical Synthesis of Polyoxometalate Based of Ionic Crystal Nanostructure: A Photocatalyst for Degradation of 2,4-dichlorophenol, *Ultrason. Sonochem*. **40**: 174–183 (2018).

[46] Benitez F.J., Beltran-Heredia J., Acero J. L., Rubio F. J., Contribution of Free Radicals to Chlorophenols Decomposition by Several Advanced Oxidation Processes, *Chemosphere*, **41**: 1271– 1277(2000).

[47] Nejad S.T., Shahrnoy A. A., Mahjoub A.R., Saloumahaleh,N. Khazaee E.Z., Photodegradation of 2,4-dichlorophenol by Supported $Pd(X_2)$ Catalyst (X = Cl, Br, N_3): a HOMO Manipulating Point of View, *Environ. Sci. Pollut. Res.* Int., **25**: 9969-9980 (2018).

[48] Buxton G., Greenstock V., Helman C. L., Ross W. P., A.B., Critical review of Rate Constants for Reactions of Hydrated Electrons, Hydrogen Atoms and Hydroxyl Radicals (•OH/O•–) in Aqueous Solution, *J. Phys. Chem. Ref. Data*, **17**: 513–886 (1988).